Upper Excited State Photochemistry: Solution and Gas Phase Photochemistry and Photophysics of 2- and 3-Cyclopropylindene[1]

Tim Waugh and Harry Morrison*

Contribution from the Department of Chemistry, Purdue University, West Lafayette, Indiana 47907

Received April 23, 1998

Abstract: The cyclopropylcarbinyl radical rearrangement has been used to probe the photochemistry and photophysics of S_2 and S_1 in 2-cyclopropylindene (**2CPI**) and 3-cyclopropylindene (**3CPI**). Studies in solution and the gas phase are described. Population of S_2 with 254 nm light excitation in the gas phase produces the anticipated ring expansion products 2,3,3a,8-tetrahydrocyclopenta[*a*]indene (**1**, $\Phi_1 = 0.1$) and 1,3,3a,8-tetrahydrocyclopenta[*a*]indene (**2**, $\Phi_2 = 0.06$) from **2CPI** and **3CPI**, respectively (Scheme 3). Direct excitation into the S_2 state (254 nm) of **2CPI** in solution also produces compound **1**. The efficiency of the solution phase chemistry is a function of excitation wavelength ($\Phi_1 = 0.022$ and 0.006 for 254 and 280 nm, respectively). The solution phase excitation spectrum of **2CPI** shows an anomalous dependency on monitoring wavelength which is attributed to a conformational equilibrium. The S_1 singlet lifetimes of the cyclopropylindenes are quite short (0.39 and 1.0 ns for **2CPI** and **3CPI**, respectively) relative to the previously measured values for the corresponding methylindenes (2.3 and 13.9 ns). These shortened lifetimes are attributed to cyclopropyl ring opening in S_1 with rates of 2.1×10^9 and 9.2×10^8 s^{-1} for **2CPI** and **3CPI**, respectively. Semiempirical excited state calculations support descriptions of the S_2 and S_1 states of alkylindenes as biradicals.

Introduction

Alkylindenes are a remarkably fruitful class of substrates for photochemical study, since they exhibit an unusual skeletal rearrangement in solution from S_1 and a novel series of hydrogen and/or alkyl shifts from S_2 in the gas phase.[2,3] Related chemistry is observed with dihydronaphthalenes.[4] The $S_0 \rightarrow S_2$ transition for these indenes and dihydronaphthalenes is centered at ca. 260 nm, while the λ_{max} for $S_0 \rightarrow S_1$ is ca. 290 nm.[3,4] As shown in Scheme 1, irradiation into the S_1 *or* S_2 states of alkylindenes *in solution* results in a net transposition of carbons 1 and 2. The reaction involves sequentially a [2 + 2] cycloaddition, a [1,3] sigmatropic shift, a retro [2 + 2] ring opening to the isoindene, and a [1,5] hydrogen shift from C2 to C1 or C3. Shown in Scheme 1 are also the reaction quantum efficiencies.

Population of the S_2 state of alkylindenes *in the vapor phase* results in the formation of solution phase products plus additional alkyl and hydrogen shift products. Excitation into S_2 in the vapor results in virtually no S_1 fluorescence, in contrast to the facile S_1 emission produced in solution. Introduction of an inert gas (butane) quenches formation of the additional alkyl/hydrogen shift products and restores fluorescence, while retaining the transposition product. On the basis of these data and the published emission spectral characteristics of styrene derivatives,[5] a mechanism unique to the gas phase was proposed which

Scheme 1. Proposed Mechanism of the Methylindene Transposition Reaction

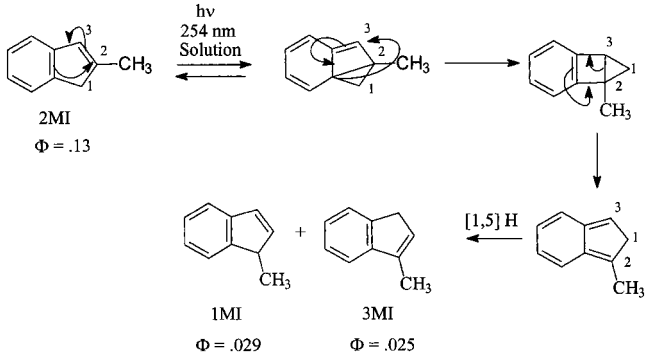

invoked conversion of the alkene into a 1,2-biradical as the chemical manifestation of either S_2 or S_1^{vib}. Multiple, sequential 1,2 shifts could then explain the scrambling observed in the products (see Scheme 2).

Recent ab initio calculations on indene[8] indicate that the S_2 state possesses a frequency mode that involves displacement

(1) Organic Photochemistry. Part 116. Part 115: Morrison, H.; Lu, Y.; Carlson, D. *J. Phys. Chem. A* **1998**, *102*, 5421−5432.

(2) (a) Morrison, H.; Palensky, F. *J. Am. Chem. Soc*. **1977**, *99*, 3507−3508. (b) Morrison, H.; Giacherio, D. *J. Am. Chem. Soc*. **1978**, *100*, 7109−7110. (c) Morrison, H.; Giacherio, D.; Palensky, F. J. *J. Org. Chem*. **1982**, *47*, 1051−1058. (d) Morrison, H.; Giacherio, D. *J. Org. Chem*. **1982**, *47*, 1058−1063.

(3) (a) Suarez, M. L.; Duguid, R. J.; Morrison, H. *J. Am. Chem. Soc*. **1989**, *111*, 6384−6391. (b) Duguid, R. J.; Morrison, H. *J. Am. Chem. Soc*. **1991**, *113*, 3519−3525.

(4) (a) Duguid, R. J.; Morrison, H. *J. Am. Chem. Soc*. **1991**, *113*, 1265−1271. (b) Duguid, R.; Morrison, H. *J. Am. Chem. Soc.* **1991**, *113*, 1271−1281.

(5) Styrene derivatives exhibit dual fluorescence that has been attributed to emission from a low energy, short-lived, planar S_1 species and a higher energy, longer lived species having twisted π bond character.[6] An analogy was drawn between this latter species and the biradical S_2 state of indene proposed by Suarez.[3a] Subsequent theoretical studies[7] have characterized the twisted species as a combination of triplet ethylene and triplet benzene and located this state 16 kcal mol^{-1} higher in energy than the planar minimum. This state is described as "a combination of triplet quinoid benzene with triplet ethylene coupled to a singlet overall." [7]

(6) (a) Steer, R. P.; Swords, M. D.; Crosby, P. M.; Phillips, D.; Salisbury, K. *Chem. Phys. Lett.* **1976**, *43*, 461−464. (b) Ghiggino, K. P.; Phillips, D.; Salisbury, K.; Swords, M. D. *J. Photochem.* **1977**, *7*, 141−146. (c) Ghiggino, K. P.; Hara, K.; Mant, G. R.; Phillips, D.; Salisbury, K.; Steer, P.; Swords, M. D. *J. Chem. Soc., Perkin Trans. 2* **1978**, 88−91.

(7) Bearpark, M. J.; Olivucci, M.; Wilsey, S.; Bernardi, F.; Robb, M. A. *J. Am. Chem. Soc*. **1995**, *117*, 6944−6953.

(8) Zilberg, S.; Kendler, S.; Haas, Y. *J. Phys. Chem*. **1996**, *100*, 10869−10874.

10.1021/ja981397y CCC: $18.00
Published on Web 03/17/1999

Scheme 2. Proposed Biradical Mechanism for Methylindene Rearrangements in the Gas Phase

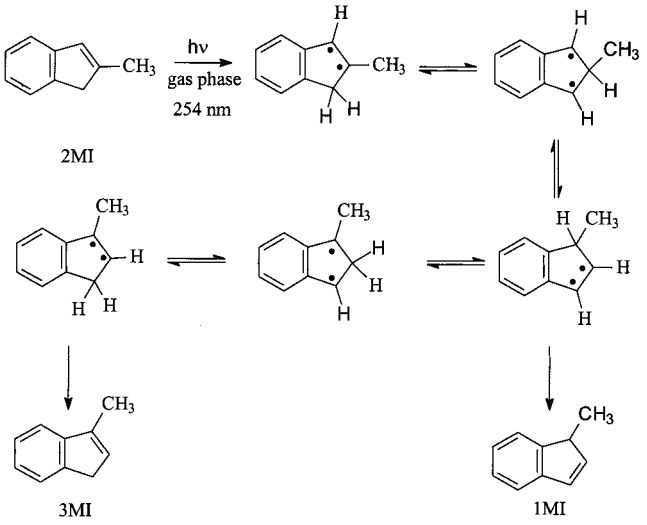

of carbons 1, 2, and 3 out of the molecular plane, an observation noted by the authors as being consistent with the characterization of S_2 as a biradical.

The intent of the current study was to provide more direct evidence for such a biradical intermediate. The facile rearrangement of cyclopropylcarbinyl radicals has proven useful in this regard and has been used to probe both thermal[9] and photochemical[10] reactions. In particular, Caldwell and Zhou[10c] used the cyclopropylcarbinyl radical clock reaction to test the model of triplet alkenes as 1,2 biradicals. Substrates studied by these workers included *cis*- and *trans*-*β*-cyclopropylstyrene, α-cyclopropylstyrene, α-cyclopropylindene (i.e., 3-cyclopropylindene, **3CPI**), and *β*-cyclopropylindene (i.e., 2-cyclopropylindene, **2CPI**). The indene triplets were created using thioxanthone and xanthone photosensitization, and the 1,3-biradicals formed by cyclopropyl ring opening were observed by transient spectroscopy. The rate constants for ring opening were measured as 3.5×10^6 and $>5 \times 10^8$ s^{-1} for **3CPI** and **2CPI**, respectively. No direct photolysis of these substrates was reported.

We have therefore prepared **2CPI** and **3CPI** and studied the solution and gas phase photophysics and photochemistry of these molecules. The anticipated photoproducts included those resulting from the transposition reaction outlined in Scheme 1 and the ring expansion products, **1** and **2**, shown in Scheme 3.

Results

Photophysics of 2CPI and 3CPI. Absorption, fluorescence, and fluorescence excitation spectra were recorded for the two cyclopropylindenes. Unless otherwise noted, the spectra were recorded at room temperature (ca. 25 °C). These data, together with reference data for the corresponding 2- and 3-methylindenes (**2MI**, **3MI**) and 2-isopropylindene (**2ISOI**), are compiled in Table 1. The solution phase spectra of the methyl- and cyclopropylindenes are displayed in Figures 1 and 2. The fluorescence and excitation spectra were multiplied by scalars to normalize them to the same scale as the absorption spectra.

(9) For some representative examples, see: (a) Griller, D.; Ingold, I. U. *Acc. Chem. Res.* **1980**, *13*, 317−323. (b) Effio, A.; Griller, D.; Ingold, I. U.; Beckwith, A. K. J.; Serelis, A. J. *J. Am. Chem. Soc.* **1980**, *102*, 1734−1736.

(10) Some selected examples: (a) Smart, R. P.; Peelen, T. J.; Blankespoor, R. L.; Ward, D. L. *J. Am. Chem. Soc.* **1997**, *119*, 461−465. (b) Hu, S.; Neckers, D. C. *J. Org. Chem.* **1997**, *62*, 755−757. (c) Caldwell, R. A.; Zhou, L. *J. Am. Chem. Soc.* **1994**, *116*, 2271−2275. (d) Rudolph, A.; Weedon, A. C. *Can. J. Chem.* **1990**, *68*, 1590−1597.

Scheme 3. Potential Ring Expansion Products from the Gas Phase Photolyses of **2CPI** and **3CPI**

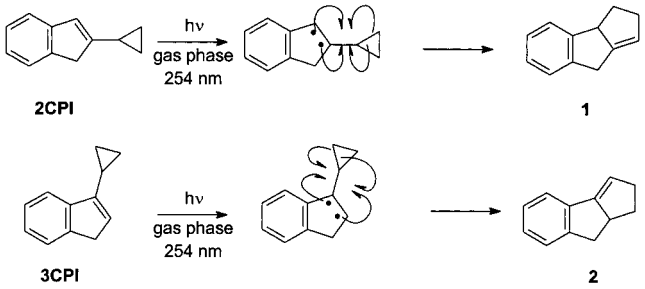

Table 1. Photophysical Data of the Indenes Studied[a]

indene	abs λ_{max}, nm (log ϵ_{max})	fluor λ_{max} (nm)	Φ_f (soln) ($\times 10^{-3}$)	τ_f (ns)	k_f ($\times 10^6$)
3MI (soln)	252 (4.00)	307	77[b]	13.9[b]	5.5[b]
3MI (gas)	248 (3.91)				
3CPI (soln)	253 (3.96)	311	4.7 ± 0.3[c]	1.0 ± 0.06[c]	4.7[c]
3CPI (gas)	248 (3.99)				
2MI (soln)	257 (4.07)	312[d]	24[b]	2.3[b]	10.4[b]
			23 ± 0.3[c]	2.4 ± 0.1[c]	9.6[c]
2MI (gas)	250 (4.15)	319[f]			
2CPI (soln)	264 (4.21)	334[d]	2.4 ± 0.2	0.39 ± 0.04[c]	9.7[c]
			3.8 ± 0.2[c]		
2CPI (gas)	253 (4.07)	331[e]			
2ISOI (soln)	258 (4.07)	312	20 ± 0.2	2.5 ± 0.1[c]	8.0[c]

[a] Unless otherwise noted, spectra were acquired in cyclohexane at 25 ± 1 °C with 254 nm excitation. [b] See ref 2c. [c] 266 nm excitation. [d] As can be seen in Figure 1, the apparent Stokes shift for **2CPI** relative **2MI** is exaggerated by using λ_{max}. The midpoints of the broad maxima in solution come at 328 and 319 nm for **2CPI** and **2MI**, respectively. [e] The midpoints of the broad maxima in the gas phase come at 335 and 319 nm for **2CPI** and **2MI**, respectively.

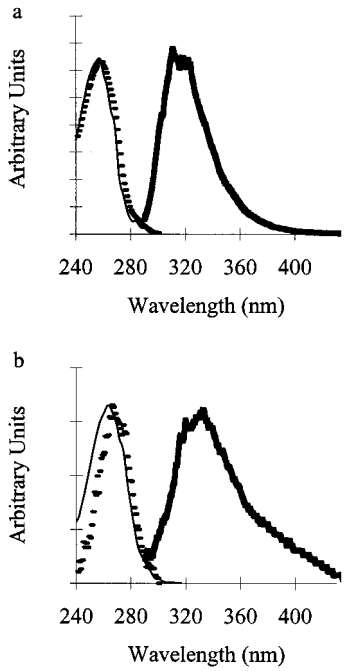

Figure 1. Solution phase absorption (thin line), fluorescence (bold line; $\lambda_{exc} = 254$ nm), and excitation (dashes; λ_{em} = fluor λ_{max}) spectra of (a) **2MI** and (b) **2CPI**.

The excitation spectra were obtained monitoring at the fluorescence λ_{max}. It is noteworthy that the excitation spectra for both **2CPI** and **3CPI** are slightly red-shifted relative to the absorption spectra. This is clearly not the case for the methylindenes.

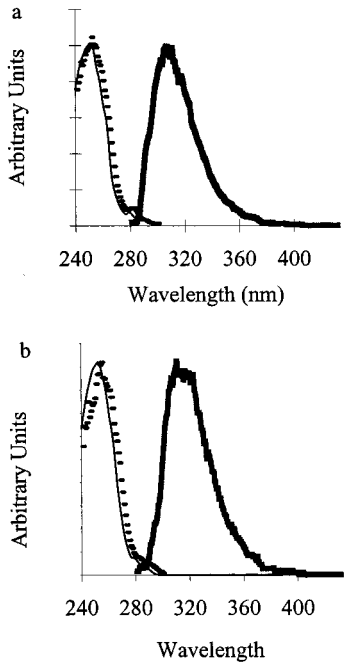

Figure 2. Solution phase absorption (thin line), fluorescence (bold line; $\lambda_{exc} = 254$ nm), and excitation (dashes; λ_{em} = fluor λ_{max}) spectra of (a) **3MI** and (b) **3CPI**.

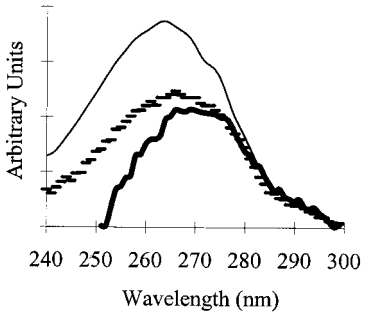

Figure 3. Comparison of the solution phase absorption spectrum (thin line) of **2CPI** with its solution phase excitation spectra monitored at 310 nm (dashes) and 330 nm (bold line).

The solution phase excitation spectra of **2CPI** were also collected as a function of monitoring wavelength and were found to be wavelength dependent (see Figure 3). Note that the excitation spectra were collected monitoring sequentially at 310 nm, 330 nm, and then again at 310 nm. No difference was observed between the two spectra collected at 310 nm, indicating that there was no degradation of the emission signal in the time span of the fluorescence experiments.[11]

The excitation spectra for **2MI** and **3CPI** exhibited no such dependence on monitoring wavelength. The excitation spectrum for **2CPI** was also collected at 77 K in a methylcyclohexane glass and found to be independent of the monitoring wavelength.

The shifts in the solution phase fluorescence excitation spectra relative to the absorption spectra for the cyclopropylindenes led us to specifically examine the possible wavelength dependence of the fluorescence quantum efficiency of **2CPI** in solution. The data are presented in Table 2.

A comparison of the absorption spectra of **2CPI** and **2MI** in solution with those in the vapor phase is presented in Figure 4. The spectra for both compounds show bathochromic shifts for the solution spectra relative to those seen in the vapor phase, with the effect magnified for **2CPI**.

(11) All indenes were purified by preparative GLC prior to analysis. The UV spectra of **2CPI** before and after the fluorescence experiments were identical.

Table 2. Wavelength Dependence of Room-Temperature Fluorescence Quantum Yields of **2CPI** in Cyclohexane

excitation wavelength (nm)	Φ_f ($\times 10^{-3}$)[a]	excitation wavelength (nm)	Φ_f ($\times 10^{-3}$)[a]
254	2.4 ± 0.2	270	2.8 ± 0.1
260	2.0 ± 0.1	275	4.2 ± 0.1
266	3.8 ± 0.2	280	5.5 ± 0.5

[a] Relative to naphthalene[12] ($\Phi_f = 0.19$).[13]

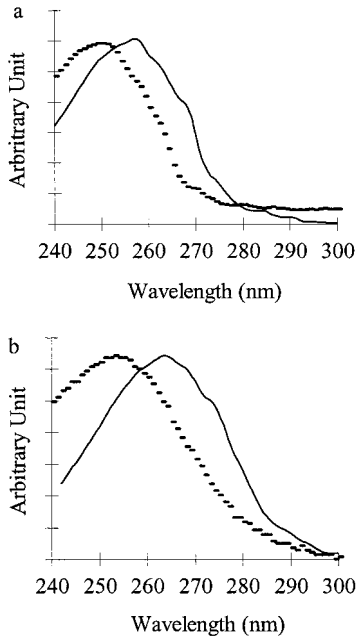

Figure 4. Comparison of the solution (thin line) and the gas-phase absorption spectra (dashes) of (a) **2MI** and (b) **2CPI**.

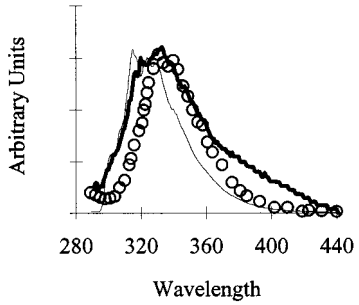

Figure 5. Comparison of the fluorescence spectra of **2CPI** ($\lambda_{exc} = 254$ nm) collected in solution at room temperature (bold line), in a glass at 77 K (thin line), and in the gas phase (circles).

In Figure 5 we compare the fluorescence spectra of **2CPI** collected in solution at room temperature, in a methylcyclohexane glass at 77 K, and in the gas phase. The low-temperature spectrum appears at the blue edge of the room-temperature fluorescence while the gas phase fluorescence spectrum is red-shifted. In contrast with **2CPI**, there is no difference between the solution and the gas phase fluorescence spectra of **2MI**.

Photolysis of 2CPI in Solution. Photolysis of **2CPI** in cyclohexane using 254 nm light gave three products as shown in eq 1. The major photoproduct is assigned as the ring expansion product **1** on the basis of its NMR and UV absorption spectra. Thus, one observes a single vinyl proton at δ 5.58, two benzylic protons at δ 3.44, and one benzylic proton appearing as a multiplet at δ 4.15−4.07. The UV spectrum is similar to

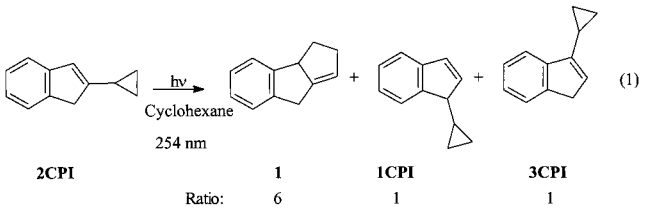

that for *o*-xylene, an indication that a double bond is no longer in conjugation with the aromatic ring.

NMR spectroscopy and a comparison of GLC retention time with authentic material have been used to identify **3CPI** as one of the minor photoproducts. The assignment of the other photoproduct as the expected transposition product, **1CPI**, is based on a comparison on its mass spectrum to the spectra of the other indene isomers. In addition to a molecular ion at *m*/*z* 156, the product shows principal fragments at 141 (loss of methyl), 128 (loss of ethylene), and 115 (loss of cyclopropyl), a pattern identical with that observed for **2CPI** and **3CPI**.

The effect of excitation wavelength on the photolysis of **2CPI** in dilute cyclohexane solutions (3−8 mM) was studied using 250, 254, 266, and 280 nm light (254 nm light was provided by a low-pressure mercury lamp, while the other wavelengths were provided by lasers). The results are presented in Table 3.

No quenching of photoproduct formation was observed in the presence of piperylene, nor are these photoproducts reported from triplet sensitization.[10c]

Photolysis of 2CPI in the Gas Phase. The photolysis of **2CPI** in the gas phase with 254 nm light typically gave two photoproducts, one of which was isolated and shown by NMR spectroscopy and GLC retention time to be the ring expansion product **1**. The second product was assigned as **1CPI** on the basis of GLC analysis. Quantum efficiencies for disappearance of **2CPI** and appearance of the products were determined using the conversion of **2MI** to **3MI** as a secondary actinometer ($\Phi_{\mathbf{3MI}} = 0.03$).[3a] The results are shown in eq 2.[14]

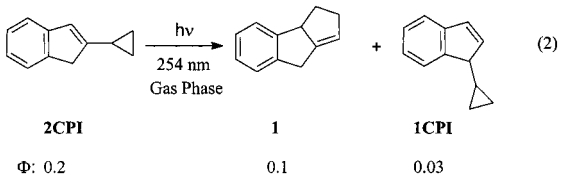

Introduction of butane into the sample chamber resulted in the appearance of **3CPI** and the formation of relatively higher levels of **1CPI**. The relative amounts of these products, as a function of butane pressure, are summarized in Table 4.

Solution Phase Photolysis of 3CPI. Prolonged photolysis of **3CPI** in cyclohexane using 254 nm light gave only a trace amount of the ring expansion product **2**. A quantum efficiency for loss of **3CPI** was measured as $\Phi_{dis} = 0.016$; a corresponding value for the formation of **2** could only be determined at high conversions and is estimated as 0.0002.

(12) For dilute solutions, the fluorescence quantum yield for naphthalene is reported to be wavelength independent over the range of wavelengths studied, see: (a) Becker, R. S.; Dolan, E.; Balke, D. E. *J. Chem. Phys.* **1969**, *50*, 239−245. (b) Birks, J. B.; Conte, J. C.; Walker, G. *J. Phys. B.* **1969**, *2*, 934−945.

(13) Birks, J. B. *Photophysics of Aromatic Molecules*; John Wiley & Sons: New York, 1969; p 126.

(14) The observed photoproducts account for ca. 65% of the loss of starting material in the gas phase photolysis. We have found evidence by GLC for the trace formation of indene in several photolyses of **2CPI**. Indene has also been found, on occasion, to be a photoproduct in the gas phase photolysis of the methylindenes. See ref 3b.

Table 3. Solution Phase Reaction Quantum Yields for the Photolysis of **2CPI** as a Function of Excitation Wavelength[a,b]

λ_{exc}	Φ_{dis} ($\times 10^{-2}$)	$\Phi_{\mathbf{1}}$ ($\times 10^{-2}$)	$\Phi_{\mathbf{3CPI}}$ ($\times 10^{-2}$)	$\Phi_{\mathbf{1CPI}}$ ($\times 10^{-2}$)
250	5.8	4.1	0.25	0.38
254	4.4 ± 0.2	2.2 ± 0.3	0.20 ± 0.04	0.25 ± 0.01
266	4.4 ± 0.3	1.8 ± 0.2	*c*	*c*
280	3.1 ± 0.3	0.6 ± 0.1	0.25[d]	0.38[d]

[a] Experiments were conducted in cyclohexane at ca. 25 °C. [b] Values without error bars correspond to only one experiment. [c] **3CPI** and **1CPI** are undetectable in these experiments. [d] The experiment was repeated in triplicate, but this product was only detected from one experiment.

Table 4. GLC Percentages of Unreacted Starting Material and of Photoproducts from the Gas Phase Photolysis of **2CPI** ($\lambda_{exc} = 254$ nm) with and without Butane

butane pressure (Torr)	% conversion[a]	unreacted **2CPI**	**1**	**3CPI**	**1CPI**	**1/1CPI**
0[b]	13−25	84	4.2		1.1	4.0
14	18	85	5.9	5.2	3.7	1.1
400	7	89	4.2	4.2	2.6	1.6
infinite[c]	5	96	3.0	0.5	0.5	6.0

[a] Photolysis times were as follows: 0 Torr, ca. 5 s; 400 Torr, ca. 15 s. [b] Indene was observed as a photoproduct in several, but not all, of the photolyses. [c] Infinite pressure corresponds to the solution phase.

Photolysis of 3CPI in the Gas Phase. Photolysis of **3CPI** vapor with 254 nm light gave the compounds shown in eq 3. The major photoproduct is assigned as the ring expansion product **2** on the basis of its NMR and UV absorption spectra. One observes a single vinyl proton at δ 5.79−5.78 split into multiplet and a multiplet at δ 2.80−2.60 corresponding to the two benzylic hydrogens. The methine proton appears as a pentet at δ 2.28−2.22 and is split by the two benzyl protons and the two methylene protons. The UV spectrum is similar to that for indene, with the two absorption maxima at 256 and 290 nm, an indication that the double bond is in conjugation with the phenyl ring. **2CPI** was identified by GLC co-injection with an authentic sample, and the identity of **1CPI** was established by co-injection of the **3CPI** gas phase reaction mixture with the reaction mixture from a solution phase photolysis of **2CPI**. Quantum efficiencies for loss of **3CPI** and formation of the photoproducts were determined using the conversion of **2MI** to **3MI**[3a] as a secondary actinometer.

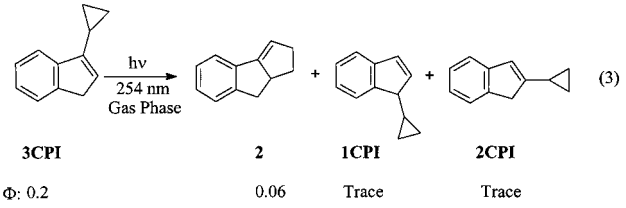

The effect of butane on the photolysis was measured, and the data are reported in Table 5. In several static photolyses we have found evidence by GLC for formation of indene.

Discussion

Major Observations. The purpose of this work was to validate the representation of upper or vibrationally excited electronic excited states of alkylindenes as biradical-like species. Consistent with our prediction, ring expansion chemistry is observed in the gas phase photolyses of **2CPI** and **3CPI**. The presence of ring expansion chemistry and the concomitant virtual elimination of transposition chemistry observed for **2CPI** in solution were unexpected. **3CPI** (like **3MI**[2c]) is essentially inert in the solution phase. Both **2CPI** and **3CPI** have shortened S_1

Table 5. GLC Percentages of Unreacted Starting Material and of Photoproducts from the Gas Phase Photolysis of **3CPI** (λ_{exc} = 254 nm) with and without Butane

butane pressure (Torr)	% conversion[a]	unreacted **3CPI**	**2**	**1CPI**	**2CPI**	**2/1CPI**
0[b]	15	93.1	3.8	2.2	0.9	1.7
8	12	86.4	3.2	4.2	3.8	0.8
18	15	99.1	0.0	0.4	0.5	0.0
infinite[c]	50	99.5	0.5			

[a] Photolysis times were as follows: 0 Torr, ca. 5 s; 18 Torr, ca. 15 s. [b] Indene was observed as a photoproduct in several, but not all, of the photolyses. [c] Infinite pressure corresponds to the solution phase.

lifetimes relative to their methyl analogues. **2CPI** exhibits a number of unusual spectral characteristics, most notable of which are absorption spectra which are phase dependent, an excitation spectrum in solution which is red-shifted relative to the absorption spectrum, and solution phase fluorescence spectra which vary with excitation wavelength.

Nature of the Excited States. The absorption spectra of styrenes, as well as the indenes studied in this work, consist of an intense short wavelength absorption band (ca. 250 nm) and a weaker longer wavelength band from 280 to 300 nm. The lower energy band corresponds to the symmetry forbidden transition to S_1 and is related to the ^1L_b transition of benzene. The higher energy band corresponds to a transition to the S_2 state and is associated with the symmetry allowed ^1L_a transition of benzene. The $S_0 \rightarrow S_2$ absorption spectrum is diffuse,[15] an indication of efficient nonradiative transitions.[16]

Analyzing the excited states of the substituted indenes computationally provides further insight into the nature of S_2 and S_1. Figure 6 contains MO coefficient plots of the HOMO-1, HOMO, LUMO, and LUMO+1 for **2CPI** in an s-trans conformation (see further discussion of the conformations of **2CPI** below). These molecular orbitals are qualitatively similar to the semiempirically generated molecular orbitals of 1-phenylpropene.[17]

The MOs in Figure 6 are representative of the orbitals calculated for the range of substituted indenes discussed in this paper. Note that the HOMO has substantial π character at C2/C3 while a π^* (antibonding) relationship exists for the corresponding atoms in the LUMO. Thus, excited state configurations which incorporate a substantial percentage of a HOMO $\rightarrow$ LUMO transition would indeed be well represented as being radical-like at C2 and, to a lesser extent, at C3. This is exactly the case for the $S_0 \rightarrow S_2$ transition in all of the indenes studied, as may be seen in Table 6 (the extensive involvement of the HOMO $\rightarrow$ LUMO transition in S_2 is analogous to that found in earlier studies of 1-phenylpropene[17] and indene.[8]

As has been previously observed,[8] depopulation of the HOMO is also involved in the formation of S_1. Table 7 shows that involvement of the HOMO dominates the $S_0 \rightarrow S_1$ transition, albeit through a HOMO $\rightarrow$ LUMO+1 excitation. Likewise, there is a major component involving population of the LUMO by excitation from the HOMO-1. The net consequence is a similar, though more modest, element of biradical character created in S_1, with an overtone of net charge transfer from the double bond to the benzene ring. Thus, the S_2 state can be chemically represented as a 1,4 biradical while the S_1 state can be represented as a 1,4 biradical slightly polarized to account for the element of charge transfer (see Figure 7).

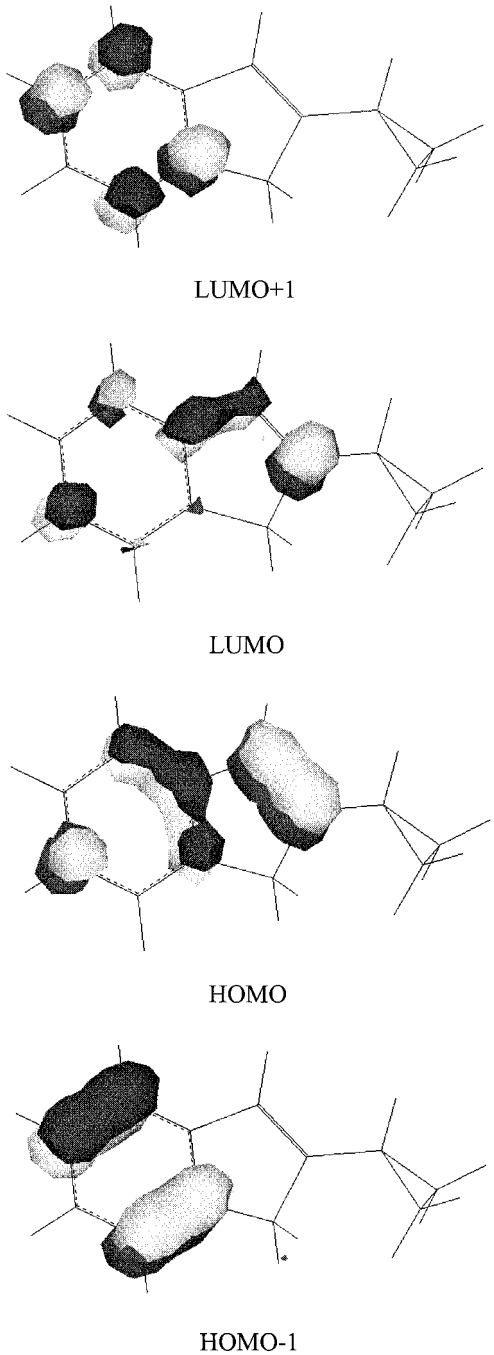

Figure 6. Molecular orbital plots of the frontier orbitals of s-trans **2CPI**.

Table 6. Percent Contribution of Singly Excited Configurations to the S_2 CI State of Substituted Indenes

indene	HOMO $\rightarrow$ LUMO	HOMO $\rightarrow$ LUMO+1
s-trans **2CPI**	90.1	6.4
3CPI	91.5	2.6
2MI	89.0	6.5
3MI	89.2	5.5
s-trans **2ISOI**	91.1	4.9

Photochemistry in the Gas Phase. A combination of isotopic scrambling and butane quenching experiments, plus the observation of minimal gas phase fluorescence, led to the proposal that three discreet species are involved in the gas phase

(15) (a) Hemley, F. J.; Leopold, D. G.; Vaida, V.; Karplus, M. *J. Chem. Phys.* **1985**, *82*, 5379−5397. (b) Zeigler, L. D.; Varotsis, C. *Chem. Phys. Lett.* **1986**, *123*, 175−181. (c) Leopold, D. G.; Hemley, R. J.; Vaida, V.; Roebber, J. L. *J. Chem. Phys.* **1981**, *75*, 4758−4769.

(16) Byrne, J. P.; Ross, I. G. *Aus. J. Chem.* **1971**, *24*, 1107−1141.

(17) Lewis, F. D.; Bassani, D. M.; Caldwell, R. A.; Unett, D. J. *J. Am. Chem. Soc.* **1994**, *116*, 10477−10485.

Table 7. Percent Contribution of Singly Excited Configurations to the S_1 CI State of Substituted Indenes

indene	HOMO → LUMO+1	HOMO-1 → LUMO
s-trans **2CPI**	60.0	28.3
3CPI	56.9	33.8
2MI	59.1	29.9
3MI	55.4	34.7
s-trans **2ISOI**	62.4	28.1

Figure 7. Chemical representation of the S_2 and S_1 states of **2CPI**.

photochemistry of alkylindenes.[3] Transposition chemistry occurs from lower vibrational levels of S_1 or $S_1{}^0$, hydrogen shifts from higher vibrational levels of S_1 ($S_1{}^{vib}$), and methyl shifts from either the highest vibrational levels of S_1 or from S_2. It was suggested that S_2 and $S_1{}^{vib}$ could be represented as biradical species.

Consistent with this view, we have observed that the ring expansion products **1** and **2** are indeed formed from the gas phase photolyses of both cyclopropylindenes. As with the gas phase photochemistry of alkylindenes[3] and dihydronaphthalenes,[4] **2CPI** also produces net [1,2] shift photoproducts (**1CPI** and **3CPI**) as well as traces of indene. The addition of butane (Table 4) results in a relative increase in the amount of **1CPI** and the appearance of **3CPI**. These products can arise either from a series of [1,2] alkyl and hydrogen shifts or from a skeletal rearrangement. The small amount of these one observes in solution, where only the skeletal rearrangement is expected,[2] argues strongly for the [1,2] shift mechanism in the gas phase. Interestingly, the fact that **3CPI** is formed only when butane is present is reminiscent of the gas phase photolysis of dihydronaphthalenes where, again, one observes unique products being formed in the presence of a quencher gas.[4] Apparently, collision with butane is relaxing the initially formed **2CPI** excited state to a level (presumably $S_1{}^{vib}$) that is not accessible by direct excitation and is capable of alkyl shift chemistry. Though this same species is likewise relatively more efficient in producing **1CPI**, it more effectively forms the 3-isomer than S_1 does in solution. With the more extensive collisional deactivation occurring in solution, the [1,2] shift mechanism disappears and the small, comparable, amounts of **1CPI** and **3CPI** now seen can be attributed to the skeletal rearrangement mechanism.

Solution Phase Photochemistry. The formation of ring expansion photoproducts in solution requires that S_2 is active in solution and/or that S_1 must also be capable of this chemistry. We will return to the issue of S_2 involvement below. What can certainly be said is that the greatly shortened singlet lifetimes for S_1 in **2CPI** and **3CPI** strongly indicate that this singlet is involved in the solution phase photochemistry. The question then is by what mechanism? We have already noted that the S_2 state is dominated (ca. 90%) by a HOMO → LUMO transition that, through the electronic distribution in the LUMO, in effect creates a cyclopropylcarbinyl radical at C2. Though the S_1 state likewise includes a ca. 28% contribution of a transition involving the population of the LUMO, its more modest role raises the question of whether a concerted, i.e., a [1,3] sigmatropic shift, mechanism may be operating in S_1.

In fact, there is good reason to believe this is not the case. Recognizing that $\Phi_1 = k_r{}^1\tau$ (where k_r is the rate of the rearrangement), we note that the singlet lifetime for **2CPI** (0.39 ns) is significantly reduced relative to the reported lifetime of **2MI** (2.3 ns).[2c] Since the radiative lifetimes of these two compounds are nearly identical, we conclude that the shortened fluorescence lifetime of **2CPI** is entirely a consequence of the new chemistry at C2 (k_r).[18] One can therefore calculate k_r by the expression $(\tau_{\mathbf{2CPI}})^{-1} = k_r + \sum k_I = k_r + (\tau_{\mathbf{2MI}})^{-1}$. Insertion of the lifetimes gives $k_r = 2.1 \times 10^9\ s^{-1}$ for **2CPI**. (An analogous calculation for **3CPI** yields a $k_r = 9.2 \times 10^8\ s^{-1}$). However, insertion of this k_r for **2CPI** into the quantum efficiency expression gives a calculated quantum yield of 0.82, while the measured value of Φ_1 at 266 nm is only 0.018. Clearly, a concerted process proceeding with the rate constant needed to explain the reduced lifetime is inconsistent with the low measured quantum efficiency, i.e., the majority of the excited state species must be returning nonproductively to the initial ground state. If one assumes that a photoinitiated ring expansion occurring by a 1,3 sigmatropic shift would proceed in a concerted manner,[19] we are led to conclude that S_1 reacts through a reversible[9b] cyclopropylcarbinyl homoallyl radical rearrangement that provides a nonproductive radiationless decay pathway for the cyclopropylindene excited state. The rate constants for ring opening would then be the k_r values calculated above. The somewhat slower rate for **3CPI** might be explained by the resonance stabilization of the benzylic position of the pseudo radical at C3 in S_1, akin to the explanation invoked to rationalize the slower rate of ring opening of the **3CPI** *triplet* relative to that of **2CPI**.[10c] A particularly interesting feature of the photochemistry arising from S_1 in the cyclopropylindenes is the dominance of ring expansion over transposition photochemistry. Clearly, ring opening is competing with the [2+2] ring closure necessary for transposition chemistry.

We return then to the question of a possible role for S_2 in the solution phase photochemistry. There are two sets of observations that could, in the absence of other data, be interpreted as support for ring opening occurring from S_2. First, the observations that the excitation spectra of the cyclopropylindenes are red-shifted relative to the absorption spectra (Figure 1) and that Φ_f therefore increases with longer wavelength excitation (Table 2) raise the possibility that S_2 is incompletely communicating with S_1. This could clearly be a result of competing photochemistry in the upper excited state. Second, there is a decrease in photochemical quantum efficiency for **2CPI** on the red-edge of its absorption (i.e., in the potential region of the $S_0 \rightarrow S_1$ transition) (cf. Table 3). One is tempted to attribute the effect to more efficient chemistry arising from S_2 relative to S_1. However, there are experimental data and literature precedents that provide an additional perspective involving the existence of conformational isomers. These are now discussed in some detail.

Conformations of 2CPI. Numerous computational[20] and experimental[21] studies have determined that the ground state energy surface of vinylcyclopropane contains two higher energy minima corresponding to an enantiomeric pair of gauche

(18) The nearly identical lifetimes of the isopropyl- and the methylindenes indicate that the diminution in the singlet lifetime of **2CPI** is due to the presence of the cyclopropane ring.

(19) It is possible that the reaction coordinate for the [1,3] sigmatropic shift involves a conical intersection that allows the excited state to decay unproductively to the **2CPI** ground state. Future theoretical analyses in collaboration with Professor Yehuda Haas of the Hebrew University are in progress. The involvement of conical intersections on the excited state surface of indene has been previously discussed, see: Bearpark, M. J.; Bernardi, F.; Olivucci, M.; Robb, M. A. *J. Phys. Chem.* **1997**, *101*, 8395−8401.

(20) (a) Klahn, B.; Dyczmons, V. *J. Mol. Struct. (THEOCHEM)* **1985**, *122*, 75−94. (b) Huang, M.-B.; Pan, D.-K. *J. Mol. Struct. (THEOCHEM)* **1984**, *108*, 49−58.

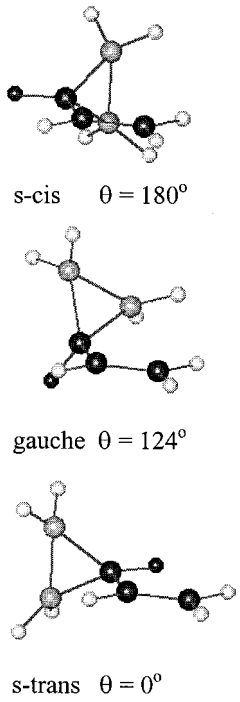

Figure 8. Structures of the rotamers of vinylcyclopropane. The torsion angles (θ) are defined by the atoms in black.

rotamers, a lower energy minimum corresponding to the s-trans rotamer, and an energy maximum corresponding to the s-cis rotamer. Figure 8 presents the structures of these rotamers. The calculated and experimental energy differences between the s-trans and gauche rotamers are 5.17 kJ/mol[20a] and 5.98,[21c] respectively.

The s-trans and gauche rotamers are known to have markedly different photochemical and photophysical properties. For example, Jorgenson[22] and Mazzocchi[23] have argued that in the photoinduced vinylcyclopropane−cyclopentene rearrangement, cyclopentene formation preferentially occurs from the gauche conformation. In contrast, the auxochromic effects of the cyclopropyl group on the UV spectra of cyclopropyl ketones and olefins are maximized in the s-trans conformation.[24,25] Conformationally rigid molecules containing a vinylcyclopropane moiety which approximate the s-trans rotamer have their UV absorption band (λ_{max} = 201.0 nm, ϵ = 14 850) shifted to the red of those compounds which model the gauche rotamer (λ_{max} = 193.0 nm, ϵ = 8740).[25] In addition, the s-trans conformer manifests itself in the chemical shifts of protons which are affected by the shielding of the cyclopropyl ring. In a study of the proton NMR spectra of 2-propenylcyclopropane and 1-methyl-2-propenylcyclopropane, Schrumpf[26] observed that the resonances for the allylic protons of 2-propenylcyclopropane appear at higher frequencies relative to those of typical allylic protons. The upfield shift was explained by postulating that the dominant rotamer is s-trans, in which the allylic hydrogens lie above the cyclopropyl ring. No such effect was seen for the allylic proton resonances of the 1-methyl analogue, where the methyl group is thought to destabilize the s-trans rotamer relative to the gauche form. Mazzocchi[23] used proton NMR to determine the s-trans to gauche conformer ratio for *trans*-2-cyclopropyl-1-phenylethylene to be 3:1. These literature precedents suggest that knowledge of the conformational equilibrium in the cyclopropylindenes may likewise be critical in understanding the photochemistry and photophysics of these compounds.

Table 8. Selected Proton NMR Resonances (ppm) of **2CPI** and **2MI** at 25 and 2 °C

	solvent	T (°C)	H_1	H_2	H_3	CH_3
2CPI	$CDCl_3$	25	6.480	3.178	1.818	
2CPI	$CDCl_3$	2	6.490	3.165	1.809	
2MI	$CDCl_3$	25	6.467	3.275		2.141
2MI	$CDCl_3$	2	6.468	3.276		2.140
2CPI	hexane	25	6.389	3.098	1.737	
2CPI	hexane	2	6.397	3.083	1.746	

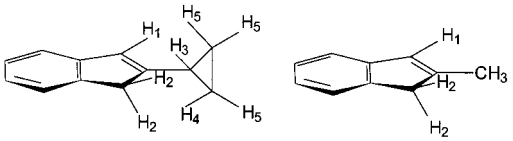

Figure 9. Numbering scheme of **2CPI** and **2MI** used for ^{1}H NMR analysis.

Ab initio calculations were therefore performed on **2CPI** at the HF/6-31G[27] level. These calculations indicate that the indene has two gauche minima, an s-trans minimum, and a maximum on the ground-state potential energy surface corresponding to the s-cis rotamer. The conformations are analogous to those shown in Figure 8. In contrast to vinylcyclopropane, the energy difference between the s-trans and gauche rotamers of **2CPI** was calculated to be 0.04 kJ/mol. At equilibrium at 298 K in the gas phase, and including entropic effects, **2CPI** is predicted to consist of 67% gauche and 33% s-trans isomers.

We have also utilized ^{1}H NMR experiments to observe the preferred conformations of **2CPI** in solution. The data given in Table 8 are consistent with the s-trans conformer being prevalent at room temperature (see Figure 9 for the numbering scheme).

We compared the 500 MHz proton NMR spectra of **2CPI** and **2MI** at 2 °C and at 25 °C. The resulting chemical shift data for several nonaromatic protons are shown in Table 8. It is evident that lowering the temperature has a minimal effect on the proton resonances of **2MI**, but a significant effect on the proton resonances of **2CPI**.[28] The fact that analogous observations were made for **2CPI** in deuteriohexane as well as deuteriochloroform indicate that the observed shifts are not solvent induced. We ascribe the shifts at lower temperatures to a progressive stabilization of the s-trans conformer. The upfield shift of the benzylic (H_2) protons would then be a result of their increased exposure to the anisotropy of the cyclopropyl ring in this conformer. The downfield shift of the vinyl H_1 resonance at lower temperature would be consistent with this interpretation.[29]

(21) (a) Traetteberg, M. *J. Mol. Struct. (THEOCHEM)*. **1988**, *189*, 357−371. (b) De Maré, G. R.; Lapaille, S. *Org. Magn. Reson*. **1980**, *13*, 75−76. (c) Carreira, L. A.; Towns, T. G.; Malloy, T. B. *J. Am. Chem. Soc*. **1978**, *100*, 385−388.

(22) Jorgenson, M. J. *J. Am. Chem. Soc*. **1969**, *91*, 6432−6443.

(23) Mazzochi, P. H.; Ladenson, R. C. *J. Chem. Soc., Chem. Commun*. **1970**, 469−470.

(24) (a) Heathcock, C. H.; Poulter, S. R. *J. Am. Chem. Soc*. **1968**, *90*, 3766−3768. (b) Pete, J. P. *Bull. Soc. Chim. Fr*. **1967**, 357−370.

(25) (a) Van-Catledge, F. A.; Boerth, D. W.; Kao, J. *J. Org. Chem*. **1982**, *47*, 4096−4106. (b) Van-Catledge, F. A. *J. Am. Chem. Soc*. **1973**, *95*, 1173−1178.

(26) Schrumpf, G. *Tetradron Lett*. **1970**, *30*, 2571−2574.

(27) (a) Hehre, W. J.; Ditchfield, R.; Pople, J. A. *J. Chem. Phys*. **1972**, *56*, 2257−2266. (b) Hariharan, P. C.; Pople, J. A. *Theor. Chim. Acta*. **1973**, *28*, 213−222. (c) Gordon, M. S. *Chem. Phys. Lett*. **1980**, *76*, 163−168.

(28) Temperature effects were also observed for protons H_4 and H_5, but the complex splitting patterns make interpretations difficult. In deuteriohexane, the **2CPI** aromatic protons' chemical shifts were observed to deviate by 0.001 ppm as a function of temperature.

(29) NOESY experiments were attempted, but H_1 and H_3 have T_1 values of 9 and 2 s, respectively. This large difference precludes the observation of a dipole−dipole interaction between the protons.

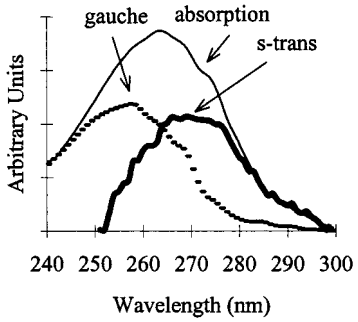

Figure 10. Hypothetical deconvolution of the solution phase UV absorption spectrum of **2CPI**. See text for definitions of the convolutes.

We return then to the solution phase absorption and excitation spectra of **2CPI** and the wavelength dependence of the photochemistry. The fact that the solution phase excitation spectra of **2CPI** are dependent upon monitoring wavelength (while those for **2MI** are not) is consistent with the presence of one or more conformations which involve the cyclopropane ring. There is ample precedent for conformers which have different absorption and emission properties to exhibit wavelength-dependent fluorescence and excitation spectra.[30,31] The marked red-shift in the **2CPI** absorption spectrum, relative to that observed for **2MI** (cf. Table 1), is consistent with Van-Catledge's observations and our NMR experiments and provides further support for our conclusion that the s-trans rotamer is prevalent.

By analogy with Van-Catledge's UV spectroscopy of vinylcyclopropanes, we would expect that the absorption spectrum of gauche **2CPI** would be to the blue of the absorption spectrum for the s-trans rotamer. In fact, the greater blue shift in the gas phase absorption maximum of **2CPI** relative to solution (11 nm, Table 1), versus that observed for **2MI** (7 nm) is consistent with the gauche conformation having become prevalent in the gas phase. This interpretation of the absorption spectra is also consistent with the ground state MO calculations (see above).

Figure 10 presents the $S_0 \rightarrow S_2$ absorption band of **2CPI** in solution, together with hypothetical gauche and s-trans convolutes. The hypothetical gauche spectrum, in which the cyclopropyl group is minimally auxochromic, is approximated by the solution phase absorption spectrum of **2MI**. The hypothetical s-trans spectrum is approximated by the solution phase excitation spectrum of **2CPI** monitored at 330 nm.

Figure 10 provides us with a rationale for the observations that ring expansion chemistry in solution increases in efficiency with shorter wavelength excitation (cf. Table 3). Such wavelengths of light would preferentially excite more of the gauche rotamer, the rotamer that has been shown to be generally more efficient in ring expansion chemistry (see above). The greater efficiency of ring expansion in the gas phase (relative to solution) can also be partially attributed to the greater gauche population in the gas phase.

The excitation spectrum of **2CPI** collected at 77 K in a methylcyclohexane glass is not dependent upon monitoring wavelength, an indication that only a single rotamer is present. In a related system, Nijveldt[32] determined that the X-ray structure of vinylcyclopropane at 100 K "slightly deviates" from the s-trans structure. By analogy with Nijveldt's work, we conclude that, at 77 K, the conformation could be a modestly deformed s-trans rotamer. In such a case, the conjugation of the cyclopropane with the indene would be reduced, resulting in hypsochromicity and hypochromicity in the excitation spectra. Table 9 summarizes our conclusions concerning the ground state conformational equilibria of **2CPI** in the three phases studied in this work.

Table 9. Summary of the Conformational Equilibrium for **2CPI**

phase	experimental observation	qualitative equilibrium
gas	MO calculations	s-trans ⇄ gauche
	UV spectrum ($\lambda_{max} = 257$ nm)	
solution	^{1}H NMR spectra	s-trans ⇆ gauche
	Wavelength dependent excitation spectra for S_1 emission	
	UV spectrum ($\lambda_{max} = 264$ nm)	
glass	Wavelength independent excitation spectra	deformed s-trans ← gauche

A comment about the positions of the S_2 and the S_1 transitions of 2CPI is in order. The solution phase absorption and excitation spectra of **2CPI**, and the wavelength dependence of the photochemistry, involve changes in quantum efficiencies that culminate in a maximal effect at 280 nm (Tables 2 and 3). The wavelength effects that fall clearly within the $S_0 \rightarrow S_2$ transition (i.e., 250−266 nm) are nicely explained by the existence of a mixture of conformational isomers. The specific maximum for Φ_f, and minimum for Φ_1, with 280 nm excitation deserves more comment. If 280 nm corresponds to excitation of the red edge of the $S_0 \rightarrow S_2$ transition, then one can assume that S_2 is not, in of itself reactive, but rather uniformly decays through S_1. However, if 280 nm excitation corresponds to the $S_0 \rightarrow S_1$ transition, then the data of Tables 2 and 3 can only be rationalized by assuming that S_2 is reacting in solution and, in fact, doing so more efficiently than S_1. This would explain the higher reaction quantum yields with 250−266 nm light, and also explain why Φ_f increases upon directly exciting into S_1. Differentiation between these two possibilities requires further spectroscopic studies.

Finally, it is interesting that the apparent Stokes shift for the absorption and emission of **2CPI** in the gas phase (82 nm) is significantly higher than that (64 nm) observed in solution (Table 1). The solution value is similar to those observed for **2MI** in both the solution and gas phases (62 and 69 nm, respectively). Large Stokes shifts are normally associated with the conversion of a state created by a Franck−Condon transition into one in which a substantial geometric change has occurred. The result is red-shifted radiative decay to a high-energy ground state species. Examples include the formation of twisted intramolecular charge transfer states (TICT)[33,34] through adiabatic processes, which have been termed horizontal radiationless transitions.[35] One may speculate that the large apparent Stokes shift for **2CPI** in the gas phase involves such an adiabatic formation of an emissive, higher energy rotamer (possibly the s-cis rotamer).

Conclusion

Excitation of **2CPI** and **3CPI** in the gas and solution phases results in cyclopropane ring opening and shortened singlet

(30) Haas, E.; Fischer, G.; Fischer, E. *J. Phys. Chem.* **1978**, *82*, 1638−1643.
(31) Lewis, F. D.; Yoon, B. A.; Arai, T.; Iwasaki, T.; Tokumaru, K. *J. Am. Chem. Soc.* **1995**, *117*, 3029−3036.
(32) Nijveldt, D.; Vos, A. *Acta Crystallogr., Sect. B: Struct. Sci.* **1988**, *B44*, 281−289.
(33) (a) Rettig, W. *Angew. Chem., Int. Ed Engl.* **1986**, *25*, 971−988. (b) Rettig, W. *Topics Curr. Chem.* **1994**, *169*, 254−299.
(34) (a) Grabowski, Z. R.; Dobkowski, J. *Pure Appl. Chem.* **1983**, *55*, 245−252. (b) Rotkiewicz, K.; Grellmann, K. H.; Grabowski, Z. R. *Chem. Phys. Lett.* **1973**, *19*, 315−318.
(35) Birks, J. B. *Chem. Phys. Lett.* **1978**, *54*, 430−434.

lifetimes. Isolation of ring expansion products in the gas phase provides evidence of a biradical reactive state, the origin of which is either S_2 or S_1^{vib}. There is also unexpected ring expansion chemistry of **2CPI** in solution, accompanied by a significant diminution in transposition chemistry. This suggests that S_1 also has diradical character. Rates of ring opening in S_1 in solution are 2.9×10^9 and 9.2×10^8 s^{-1} for **2CPI** and **3CPI**, respectively. The photochemistry and photophysics of **2CPI** are governed by an s-trans ⇌ gauche conformational equilibrium, with ring expansion likely to be occurring preferentially from the gauche rotamer. This rotamer dominates the equilibrium in the gas phase, while the s-trans rotamer is prevalent in solution. The wavelength-dependent effects observed for photochemistry and fluorescence of **2CPI** in solution are consistent with either S_2 decaying to S_1 prior to reaction or emission or S_2 photochemistry competing with internal conversion to the lower excited state.

Experimental Section

Materials. Diethyl ether was dried over sodium/benzophenone prior to use. Cyclopropyl bromide (Aldrich, Lancaster), 1-indanone (Aldrich), and iodomethane (Aldrich) were used as received. 2-Indanone (Aldrich) was purified by flash chromatography (CH_2Cl_2) and recrystallized from hexane. Spectranalyzed cyclohexane (Fisher) was used for all spectroscopic and photochemical studies. Naphthalene was purified by the method of Perrin.[36] (*E*)-1-Phenyl-2-butene (Aldrich) was purified by GLC prior to use.

Instrumentation. ^{1}H and ^{13}C NMR spectra were obtained using Varian Gemini 200 MHz or Varian 500 MHz spectrometers. Chemical shifts are reported in deuteriochloroform in parts per million relative to tetramethylsilane (TMS) or residual chloroform. For the variable-temperature ^{1}H NMR experiments GLC pure **2CPI** and **2MI** was dissolved in deuteriochloroform or deuteriohexane and analyzed at 2 and 25 °C utilizing the Varian 500 MHz spectrometer equipped with a cryostatically controlled temperature unit. These samples were ca. ≤5% v/v in the solvents used.

Mass spectra were recorded on a Finnigan 4000 mass spectrometer interfaced to a gas chromatograph containing either packed or capillary columns. Electron impact (EI) and chemical ionization (CI) mass spectra were recorded at 70 eV. High-resolution mass spectra were recorded on a Kratos Model MS-50 instrument operated at 70 eV for EI. Ultraviolet absorption spectra were collected in matched 1 cm^2 quartz cells using a Cary 100 spectrometer interfaced to a Pentium 100 MHz PC controlled by the Cary Scan Package software. Corrected steady state fluorescence and excitation spectra were recorded on an SLM Aminco Model SPF-500 C spectrofluorometer using the A/B mode in all experiments. Low-temperature fluorescence spectra were collected using a liquid nitrogen cooled Dewar equipped with a quartz window. Analytical GLC was performed on Varian Model 3700 FID and Varian Model 3500 FID capillary gas chromatographs with Hewlett-Packard 3390A digital integrators. Preparative GLC was performed on a Varian Model 3300 TCD gas chromatograph with a Hewlett-Packard 3390A digital integrator. Two columns were used: A (J & W DB-1, 15 m × 0.25 mm id., 0.25 μm) and B (10 ft × 0.25 in, 5% OV-17 on Chromosorb W).

Computations. Excited state calculations were performed using the HyperChem 5.0 (Hypercube Inc.) program package. Geometries of the indenes were optimized in C_s symmetry using the AM1[37] or ZINDO/1[38] Hamiltonians. The molecular orbital plots were generated from ZINDO/S-CI[39] calculations using 20 occupied and 20 unoccupied orbitals. The multiplicity of each eigenvector (excited state) was determined from the state dipole moments. All the single determinant wave functions comprising each eigenvector were identified from the calculated UV spectrum. The 400 electron spin up, singly excited configurations contributing to each wave function were identified from the CI matrix, squared, multiplied by 2 (to account for the spin down electrons), and multiplied by 100 to convert to a percentage.

Ground-state MO calculations were conducted using Gaussian 94.[40] All geometries were optimized at the HF/6-31G[27] level of theory. Frequency calculations at this level showed the s-trans and gauche rotamers to be minima while the s-cis rotamer was shown to be a maximum. Energy differences between the conformers are the HF energies.

Solution Phase Photochemistry. Experiments were done with matched quartz tubes (1 cm o.d.) in a Rayonet Model RPR-100 reactor (New England Ultraviolet Company) equipped with two or four 254 nm low-pressure mercury lamps or with laser light sources. Quantum efficiencies at 254 nm were measured using 1-phenyl-2-butene actinometry[41] with column A (80 °C) to analyze the *E*/*Z* isomerization. The *E* isomer (Aldrich) was purified by GLC using column B (100 °C). All solution experiments were conducted in cyclohexane and degassed with argon for 30 min prior to photolysis. Photolyses conducted at 266 nm were performed using a Continuum NY-61 Nd:YAG laser equipped with a frequency quadrupler (10 Hz, 3.0−3.3 mJ/pulse). Irradiations at 280 and 250 nm employed a YAG-pumped dye laser (Continuum ND-60, Rhodamine 590 or Coumarin 500, respectively). A 2× beam enlarger was used in front of the photolysis cell to avoid cell damage. Singlet lifetimes were collected using either a time-correlated photon counting apparatus with 266 nm excitation from a frequency quadrupled mode locked Quantronix Nd:YAG laser with a pulse width of fwhm 120 ps or using a PTI LS-1 spectrophotometer exciting with either 254 or 266 nm light.

Gas Phase Photochemistry. The apparatus has been described in detail elsewhere.[3a] Exploratory and preparative experiments were performed under flowing conditions. Briefly, a liquid sample was distilled (typically at pressures of 20 mTorr at 25 °C) through a quartz tube (33 cm in length × 14.7 cm in circumference) surrounded by sixteen 254 nm low-pressure mercury lamps. The photolyzed vapor was collected in a liquid nitrogen trap. After warming to room temperature, the trap was washed twice with 10 mL of pentane and the combined washings were concentrated under a stream of nitrogen. Exploratory experiments utilized 10−20 mg of the appropriate indene, while preparative work employed 30−300 mg. Isolation of photoproducts employed either silica gel chromatography (hexane as eluent) or separation by GLC using column B.

Qualitative and quenching studies were performed under static conditions which involved filling a cylindrical quartz vessel (length 34 cm × 4.7 cm o.d.) with the desired vapor to pressures of 150−800 mTorr, depending on the indene. Unless otherwise noted, the pressures were not corrected for instrument response. The vessel was removed from the vacuum line and placed in a modified RPR-100 Rayonet reactor containing one 254 nm lamp for photolysis times of 5−15 s at 25 °C. Collection of the photolyzed sample required immersion of the vessel in liquid nitrogen and the injection of 5 mL of pentane containing an internal standard. After the vessel warmed to room temperature, the solution was removed and the vessel was again washed with pentane. The combined pentane washings were concentrated under a stream of nitrogen and analyzed on column A (120 °C). The gas phase apparatus was designed with apertures to allow the introduction of a

(36) Perrin, D. D.; Armarego, W. L. F.; Perrin, D. R. *Purification of Laboratory Chemicals*, 2nd ed.; Pergamon Press: New York, 1980; pp 349−350.

(37) Dewar, M. J. S. *J. Am. Chem. Soc*. **1985**, *107*, 3902−3909.

(38) (a) Bacon, A. D.; Zerner, M. C. *Theor. Chim. Acta*. **1979**, *53*, 21−54. (b) Anderson, W. P.; Edwards, W. D.; Zerner, M. C. *Inorg. Chem*. **1986**, *25*, 2728−2732.

(39) (a) Ridley, J.; Zerner, M. C. *Theor. Chim. Acta* **1973**, *32*, 111−134. (b) Ridley, J.; Zerner, M. C. *Theor. Chim. Acta* **1976**, *42*, 223−236. (c) Zerner, M. C.; Loew, G. H.; Kirchner, R. F.; Mueller-Westerhoff, U. T. *J. Am. Chem. Soc*. **1980**, *102*, 589−599.

(40) M. J. Frisch, M. J.; Trucks, G. W.; Schlegel, H. B.; Gill, P. M. W.; Johnson, B. G.; Robb, M. A.; Cheeseman, J. R.; Keith, T.; Petersson, G. A.; Montgomery, J. A.; Raghavachari, K.; Al-Laham, M. A.; Zakrzewski, V. G.; Ortiz, J. V.; Foresman, J. B.; J. Cioslowski, J.; Stefanov, B. B.; Nanayakkara, A.; Challacombe, M.; Peng, C. Y.; Ayala, P. Y.; Chen, W.; Wong, M. W.; Andres, J. L.; Replogle, E. S.; Gomperts, R.; Martin, R. L.; Fox, D. J.; Binkley, J. S.; Defrees, D. J.; Baker, J.; Stewart, J. P.; Head-Gordon, M.; Gonzalez, C.; Pople, J. A. Gaussian, Inc.: Pittsburgh, PA, 1995.

(41) Morrison, H.; Pajak, J.; Peiffer, R. *J. Am. Chem. Soc*. **1971**, *93*, 3978−3985.

quencher gas (butane). Samples were degassed prior to flowing and static experiments by at least five freeze−pump (5 mTorr)−thaw cycles. Gas phase absorption and fluorescence studies utilized two modified matched 1 cm^2 rectangular fluorescence cells fitted with vacuum attachments.

Syntheses. 2-Cyclopropylindene (**2CPI)** and 3-cyclopropylindene (**3CPI)** were synthesized following the literature procedure and spectral assignments were consistent with published data.[7c] **2CPI**: MS (EI) *m*/*z* (relative intensity) 156 (M^+) (100), 141 (84.89), 128 (41.03), 115 (64.36). **3CPI**: MS (EI) *m*/*z* (relative intensity) 156 (M^+) (88.29), 141 (100), 128 (43.66), 115 (96.70).

2-Methylindene (2MI). The above literature procedure was modified by using iodomethane and gave a 50% yield of **2MI**. Spectral assignments were consistent with the literature.[42]

2-Isopropylindene (2ISOI). 2-Isopropylidene-1-indanone was prepared from the aldol condensation of 1-indanone with acetone as described in the literature.[43] The reduction of the ketone with sodium borohydride in pyridine[44] afforded 2-isopropyl-1-indanol, which was dehydrated with acid to give **2ISOI**. Spectral data were consistent with those in the literature.[45]

Spectroscopy. The cyclopropyl and methylindenes were purified by preparative GC using column B (170 °C, **3CPI**: R_t 6.1 min, **2CPI**: R_t 8.5 min; 160 °C, **3MI**: R_t 3.25 min, **2MI**: R_t 3.30) prior to analysis. Relative fluorescence quantum yields of **2CPI** and **3CPI** in cyclohexane were determined with 254 nm excitation relative to toluene. The fluorescence wavelength study was conducted on **2CPI** using naphthalene as the fluorescence reference. Separate solutions of **2CPI** in cyclohexane were prepared having absorbances at 254, 260, 266, 270, 275, and 280 nm of 0.10 ± 0.01. Quantum efficiencies were corrected for differences in absorbance. Cyclohexane solutions were prepared having absorbances of ca. 0.25 at 266 nm for singlet lifetime determinations. The data were fit to first-order decay kinetics. Gas phase absorption and fluorescence spectra were collected in the modified fluorescence cells, and extinction coefficients were calculated using corrected pressures.[46]

Solution Phase Photolysis of 2CPI. Cyclohexane solutions of 3−8 mM **2CPI** were irradiated at 254 nm to yield a reaction mixture containing one major and two minor photoproducts. The solvent was removed and the residue chromatographed over silica gel (230−400 mesh) using hexane as eluent to give the ring expansion product **1**: ^{1}H NMR ($CDCl_3$, 500 MHz) δ 7.31−7.14 (m, 4H), 5.58−5.57 (s, 1H), 4.15−4.07 (m, 1H), 3.44 (s, 2H), 2.78−2.61 (m, 1H), 2.56−2.41 (m, 2H), 1.85−1.68 (pentet, 1H); ^{13}C NMR (500 MHz, $CDCl_3$) δ 150.34, 146.43, 144.76, 126.58, 126.27, 124.81, 123.80, 120.79, 55.56, 35.32, 32.42; UV (cyclohexane) λ_{max} (log ϵ) 252 (2.87), 259 (3.05), 265 (3.16), 272 (3.16); MS (EI) *m*/*z* (relative intensity) 156 (M^+) (100), 141 (47.6), 128 (64.57), 115 (31.77); HRMS (EI) calcd for $C_{12}H_{12}$ (M^+) 156.1017, found 156.1012.

A minor photoproduct was isolated using column B (170 °C) and identified by ^{1}H NMR as **3CPI**. The third photoproduct was found to be inseparable from the starting material by flash chromatography and was unobtainable in sufficient amounts for identification using preparative GC. It was assigned as **1CPI** on the basis of a comparison of its GLC mass spectrum to that of **2CPI** and **3CPI**: MS (EI) *m*/*z* (relative intensity) 156 (M^+) (72.34), 141 (36.31), 128 (43.48), 115 (100).

Solution Phase Quantum Yields. Cyclohexane solutions (3 mL) containing 3 mM **2CPI** and either 3 mM tridecane (for determining starting material disappearance) or 0.5 mM tridecane (for photoproduct formation) were placed in matched quartz tubes. Two actinometer solutions, 15 mM in cyclohexane, were placed into matched quartz tubes and used to give a time average of the flux during the course of the photolysis. The solutions were and irradiated in the Rayonet reactor using four 254 nm lamps for 5 min. Solution quantum yields for **3CPI** were determined in like fashion. For laser studies, sample solutions in cyclohexane were placed in matched Vycor laser cells and irradiated at 250 nm for 14 min, at 266 nm for 2.7 min, and at 280 nm for 9.0 min.

Gas Phase Photolysis of 3CPI. Product **2** was isolated by silica gel chromatography: ^{1}H NMR ($CDCl_3$, 200 MHz) δ 7.44−7.42 (m, 1H), 7.26−7.15 (m, 3H), 5.79−5.78 (AB q, 1H), 3.4−3.2 (m, 1H), 3.11−3.03 (m, 1H), 2.8−2.6 (m, 2H), 2.56−2.45 (m, 1H), 2.28−2.22 (pentet, 1H), 1.69−1.45 (pentet, 1H); ^{13}C NMR (200 MHz, $CDCl_3$) δ 153.37, 150.24, 127.51, 126.53, 125.66, 121.75, 117.22, 51.69, 38.02, 36.97, 33.12; UV (cyclohexane) λ_{max} (log ϵ) 256 (3.66), 290 (2.57); MS (EI) *m*/*z* (relative intensity) 156 (M^+) (100), 141 (71.41), 128 (58.48), 115 (59.43); HRMS (CI) calcd for $C_{12}H_{13}$ (M^+ + H) *m*/*z* 157.1017, found *m*/*z* 157.1012.

Butane Quenching Studies. Using static conditions, **2CPI** vapor was distilled into the reaction vessel to a pressure of 150 mTorr and photolyzed for 5 s using one 254 nm lamp. The product mixture was analyzed by column A (120 °C) and found to contain compound **1** and **1CPI**. **2CPI** vapor was again distilled into the reaction vessel to a pressure of 150 mTorr with the addition of butane (8 and 400 mTorr) and photolyzed for 5−15 s. The product mixture was analyzed by column A at 120 °C and found to contain the ring expansion product **1**, **1CPI,** and **3CPI** in the product ratios reported in Table 4. Quenching studies were repeated for **3CPI** and the results are in Table 5.

Gas Phase Quantum Yields. Absorbances for the methyl- and cyclopropylindenes were measured in 1 cm rectangular cells and corrected for the longer optical path length of the cylindrical reaction vessel by the expression $L = \pi d/4$, where L is the effective path length of a cylinder. The fraction of light absorbed by the methylindenes was ca. 60%, while the absorbances for **3CPI** and **2CPI** were 10% and 7%, respectively. Prior to photolysis the mass of the indene vapor was determined by GLC analysis at gauge pressures of 400 mTorr for **2MI**, 800 mTorr for **3MI**, 325 mTorr for **3CPI**, and 150 mTorr for **2CPI**. These single point calibrations were precise to ±5% and were used to determine the quantum yields of disappearance. The vapor was photolyzed for 5−10 s and resulted in up to 25% loss of starting material depending on the indene. Due to the approximations made and the low absorbances, quantum yields are only reported to one significant figure.

Acknowledgment. This work was supported by the National Science Foundation Grant (Grant CHE9530650).

JA981397Y

(42) Marchal, E.; Basselier, J.-J.; Sigwalt, P. *Bull. Soc. Chim. Fr*. **1964**, 1740−1749.

(43) Plattner, P. A.; Fürst, A.; Wyss, J.; Sandrin, R. *Helv. Chim. Acta*. **1947**, *30*, 689−694.

(44) Jackson, W. R.; Zurgiyan, A. *J. Chem. Soc*. **1965**, 5280−5287.

(45) Edlund, U *Org. Magn. Reson*. **1978**, *11*, 516−519.

(46) Gauge pressure correction factors were determined using the mass of the vapor and assuming ideality. These were used to calculate the vapor concentration in the vacuum adapted fluorescence cell: 1 Torr gauge pressure = 0.4 Torr **2MI**, **3MI** calculated pressure; 1 Torr gauge pressure = 0.1 Torr **2CPI**, **3CPI** calculated pressure. Note that a correction factor of 0.67 Torr was used for the methylindenes in the previous work. See ref 3a.